ELSEVIER

Journal of Power Sources 54 (1995) 329–333

JOURNAL OF POWER SOURCES

# The $LiNiO_2$ solid solution as a cathode material for rechargeable lithium batteries

R.V. Moshtev [a], P. Zlatilova [a], V. Manev [a], Atsushi Sato [b]

[a] *Central Laboratory of Electrochemical Power Sources, Bulgarian Academy of Sciences, Sofia 1113, Bulgaria*

[b] *Chubu University, Department of Industrial Chemistry, Kasugai, Aichi-ken 487, Japan*

**Abstract**

Samples of $Li_xNi_{2-x}O_2$ ($0.91 < x < 0.99$), synthesized by the solid-state reaction between $LiNO_3$ and $Ni(OH)_2$ were characterized by X-ray diffraction, chemical analyses and electrochemical tests. A good correlation is found between $x$ and the Bragg intensity ratios $R_{(102)} = \{I_{(102)} + I_{(006)}\}/I_{(101)}$ and $R_{(003)} = I_{(003)}/I_{(104)}$. The electrochemical activity of the sample as exhibited by the discharge capacity in the first cycle is a function of $x$ with a maximum at $x = 0.97$–$0.98$. The discharge capacity of the optimized sample at a 7 h rate is strongly dependent on the end charge voltage in the range from 4.1 to 4.3 V and reaches a 220 mAh/g at $U_{max.} = 4.45$ V. The cycling stability after the first five to eight cycles is 99.88%, i.e., a capacity loss of only 0.12% per cycle.

*Keywords:* Cathode materials; Lithium; Nickel oxide; Rechargeable lithium batteries

## 1. Introduction

The competition between several cathode materials suitable for 4 V rechargeable Li batteries (Li-ion batteries) is in full development during the last three to four years. Thanks to the continuous efforts of many investigators the synthesis methods and, consequently, the electrochemical parameters of the four possible candidate materials have been significantly improved: $LiCoO_2$ [1,2], $LiNi_{1-x}Co_xO_2$ [3], $LiNiO_2$ [4–7] and $LiMn_2O_4$ [8–10]. Thus, the discharge capacity of $LiMn_2O_4$ has closely approached its theoretical value of 148 mAh/g, while those of the three other intercalation compounds vary between 140 and 170 mAh/g, depending on the cycling conditions. In contrast to $LiMn_2O_4$, the specific capacities of the first three compounds are markedly below their theoretical values, with an utilization not higher than 75%. This implies that they are subject to eventual future amelioration. This is especially true for $LiNiO_2$, for which it is well known that its electrochemical performance is strongly dependent on the stoichiometry, crystal structure and cation disorder, which could be further improved by new synthesis methods. Moreover, the recent comparative study of Ohzuku et al. [3] has given strong evidence that $LiNiO_2$ is the most promising compound in view of its higher capacity, better reversibility and lower maximum charge voltage, which does not endanger the electrolyte stability during cycling.

It seems to be generally accepted that the electrochemical characteristics of $LiNiO_2$ negative electrodes in nonaqueous rechargeable Li cells can be improved by avoiding any structural disorder, which means a Li/Ni ratio as close as possible to unity in the phase. In order to study the effect of stoichiometry on the X-ray diffraction (XRD) parameters and on the electrochemical performance of $Li_xNi_{2-x}O_2$, samples with $x$ in the 0.91–0.99 range were synthesized, investigated and characterized. An attempt was also made to correlate some XRD intensity ratios of the samples with their electrochemical parameters.

## 2. Experimental

### 2.1. Synthesis

The $LiNiO_2$ samples were synthesized in a horizontal tube furnace through the solid-state reaction between $LiNO_3$ and $Ni(OH)_2$ in alumina boats, under oxygen flow. By changing the Li/Ni ratio in the starting mixture (1.0 to 1.1), the oxygen flow rate (20 to 100 ml/min), the temperature of the final heat treatment (700–800 °C) and the time of this treatment (24–68 h) it was possible to obtain samples with different stoichiometry ($0.91 < x < 0.99$).


*SSDI* 0378-7753(94)02094-J

### 2.2. XRD measurements

The XRD measurements were performed with Cu Kα radiation on a Philips APD 15 powder diffractometer, provided with a P-830-010 computer and a software for the exact determination of the Bragg peak positions and their net integrated intensities corrected for the background. The net integrated intensities $I_p = I \sin \theta$ are directly recorded by the apparatus. The characteristic intensity ratios are calculated here with the $I_p$ values as done by Dahn et al. [5] and at difference from others authors where these ratios are calculated with $I$ values [3,6,7,11].

Step scan recording at 0.02° $2\theta$ step size and 2 s counting time were applied. The lattice parameters $c$ and $a$ were computed by the least-squares fit of the (003), (101), (102), (104) and (110) peak positions assuming a crystal lattice of the hexagonal $R3m$ s.g.

Selected samples were analyzed for Ni(III) and Ni(II) by the iodometric and complexometric titration methods to determine the oxidation state of Ni wherefrom the Li/Ni ratio and $x$ were assessed.

### 2.3. Electrochemical characterization

Cathodes for the electrochemical investigations were prepared by pressing a blend of the $LiNiO_2$ sample with 20 wt.% teflonized acetylene black on an Al foil disc, 15 mm in diameter. Typical cathodes weighed $40 \pm 3$ mg were $100 \pm 10$ μm thick and had an apparent density of $2.40 \pm 0.05$ g/cm$^3$. The cathodes were assembled in stainless-steel laboratory coin cells provided with Li counter and Li reference electrodes. The cells simulate closely the geometry of commercial coin cells, but can be easily disassembled for the inspection of the active materials after the test. Two electrolyte solutions were used: 1 M $LiClO_4$ in ethylene carbonate–propylene carbonate (1:1) and 1 M $LiPF_6$ in ethylene carbonate–dimethyl carbonate (1:1) with a water content less than 30 ppm. The cathodes were dried under vacuum at 150 °C at least for 3 h before their assembly in the cells. Cycling was performed continuously at constant current usually between 2.6 and 4.25 V at room temperature.

## 3. Results and discussion

### 3.1. XRD data

Tables 1 and 2 list experimental XRD data of a sample with $x = 0.986$ (by chemical analysis) juxtaposed to values of $2\theta$ calculated by Dahn et al. [5] for $x = 1$ and to the $I_p/I_{p(104)}$ relative net integrated intensities observed by the same authors. The good agreement between these data and the present measurements points to the accuracy of the latter.

As demonstrated by Dahn et al. [5] and later more precisely by Reimers et al. [12] the $x$ value in the $Li_xNi_{2-x}O_2$ phase san be assessed quite accurately from the XRD data. More specifically, it was established (Table 4 in Ref. [12]) that the net integrated intensity ratio $R(102) = \{I_{p(102)} + I_{p(006)}\}/I_{p(101)}$ is a linear function of $x$ in the $0.90 < x < 1.00$ range. Plots in Fig. 1 present this experimental relationship (open circles). The $LiNiO_2$ samples studied in both papers [5,12] were synthesized with LiOH as a source of Li at 600 °C, while we used $LiNO_3$ and applied temperature in the 700–800 °C range. Since the synthesis conditions could affect the $R_{(102)}$ versus $x$ dependence we checked it with our experimental values of $x$ determined by chemical analysis (full circles in Fig. 1). It can be seen that both sets of data lie closely on the same linear plot, implying that the $R_{(102)}$ versus the $x$ relationship is valid for samples obtained by both methods.

It has been demonstrated [3,7,11] that the Bragg intensity ratio $R_{(003)} = I_{(003)}/I_{(104)}$ can serve also as a reliable quantitative criterion for the stoichiometry of the $Li_xNi_{2-x}O_2$ phase. Thus, according to Ohzuku et al. [3] samples with $R_{(003)}$ from 1.32 to 1.39 exhibit high electrochemical activity. On the other hand, these authors assume that the exact chemical composition of the compound is not the main factor determining its electrochemical performance when the Li/Ni ratio is close to unity and therefore they rely rather on the XRD and electrochemical characterization to control the preparation conditions. Our experiment, however, revealed a clear linear dependence of $R_{(003)}$ versus $x$ in the $0.91 < x < 0.99$ range demonstrated in Fig. 2 (full dots). As pointed out in the experimental part, the present intensity ratios $R_{(003)}$ are estimated with the net integrated intensities $I_p = I \sin \theta$, as released directly from the computer of the diffractometer. These are different to the results reported in Refs. [3,7,11], where the $R_{(003)}$ ratio was calculated with $I$ values, not corrected for the angle of incidence $\theta$, and consequently such $R_{(003)}$ values are higher than those presented here. In order to make possible the comparison between the present results and those reported in Refs. [3,7,11] we have recalculated our data with $I$ values and plotted them as a $R'_{(003)}$ versus $x$ dependence in the same Fig. 2 (triangles). It is seen that, in agreement with the results of Ohzuku et al. [3], our samples with a higher stoichiometry ($x > 0.98$) exhibit $R_{(003)}$ values larger than 1.30.

From the data presented in Figs. 1 and 2 it can be inferred that the intensity ratio $R_{(003)}$ could be also used in assessing the stoichiometry of the $LiNiO_2$ phase.

### 3.2. Electrochemical performance

Fig. 3 displays the charge/discharge curves of a $Li_xNi_{2-x}O_2$ cathode with $x = 0.974$, cycled between 2.60

Table 1
X-ray diffraction data of $Li_xNi_{2-x}O_2$ samples with $x=0.986$

| Peak (*hkl*) | 2θ (observed) | 2θ (calculated) | *d* (Å) (observed) | $I/I_{(104)}$ (observed) | $I/I_{(104)}$ (observed in Ref. [5]) |
|---|---|---|---|---|---|
| 003 | 18.740 | 18.75 | 4.734 | 59.1 | 51 |
| 101 | 36.603 | 36.59 | 2.454 | 40.9 | 41 |
| 102 | 38.263 | 38.25 | 2.352 | 18.1 | 23 |
| 104 | 44.431 | 44.39 | 2.038 | 100 | 100 |
| 110 | 64.771 | 64.75 | 1.439 | 64.0 | 66 |

Table 2
Relevant X-ray diffraction data of $Li_xNi_{2-x}$ samples

| No. | *a* (Å) | *c* (Å)[a] | $R_{(003)}$ | $R_{(102)}$ | $x_{102}$ | $x_{analyzed}$ |
|---|---|---|---|---|---|---|
| 1 | 2.8765 | 14.188 | 0.402 | 0.645 | 0.915 | 0.912 |
| 2 | 2.8830 | 14.215 | 0.457 | 0.542 | 0.953 | 0.955 |
| 3 | 2.8818 | 14.150 | 0.511 | 0.516 | 0.962 | 0.959 |
| 4 | 2.8826 | 14.217 | 0.520 | 0.509 | 0.965 | 0.970 |
| 5 | 2.8825 | 14.176 | 0.519 | 0.505 | 0.966 | 0.966 |
| 6 | 2.8813 | 14.211 | 0.522 | 0.487 | 0.973 | 0.975 |
| 7 | 2.877 | 14.203 | 0.586 | 0.451 | 0.986 | |
| 8 | 2.879 | 14.177 | 0.591 | 0.441 | 0.989 | 0.986 |
| 9 | 2.879 | 14.192 | 0.593 | 0.441 | 0.989 | |

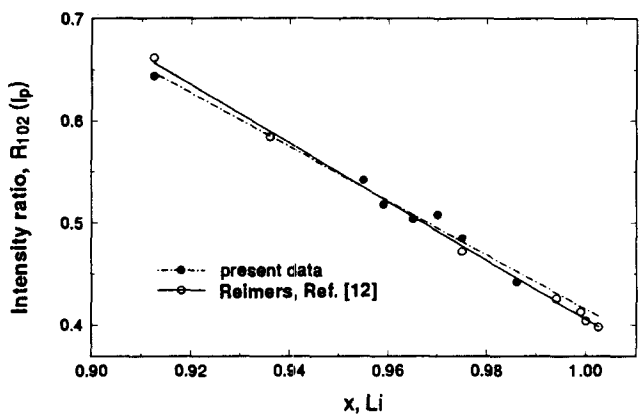


Fig. 1. Dependence of the $R_{(102)}$ Bragg intensity ratio on $x$ in the $Li_xNi_{2-x}O_2$ phase: (●) experimental data by chemical analysis, and (○) experimental data from Ref. [12].

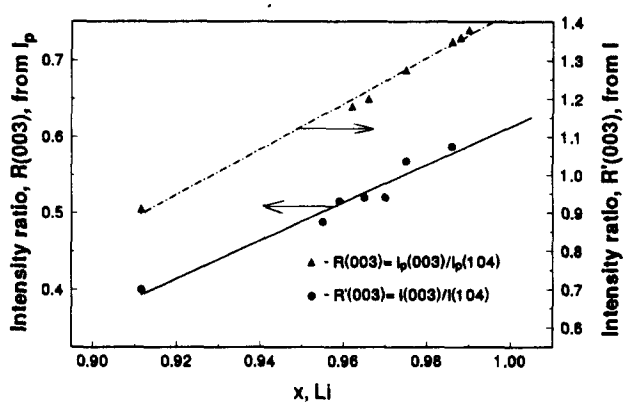


Fig. 2. $R_{(003)}$ Bragg intensity ratio as a function of $x$ in the $Li_xNi_{2-x}O_2$ phase: (●) (left ordinate) with $I_p=I\sin\theta$ values, and (○) (right ordinate) with $I$ values.

and 4.27 V at 0.51 mA/cm² or 21 mA/g of the active material in the first, second and fifth cycles. The specific capacities in the first cycle, 229 mAh/g at charge and 199 mAh/g at discharge, are some of the largest reported so far for the end charge voltage and current applied. The large discharge capacity is evidently related to the long voltage plateau between 4.22 and 4.25 V, which is characteristic for the well-synthesized samples and is not observed with samples with $x$ lower than 0.97 and higher than 0.98. The voltage drop observed upon the charge/discharge switching is comparatively small (about 100 mV) and comprises the ohmic drop in the liquid electrolyte and the diffusion polarization in the solid-ion conductor, 20 and 80 mV, respectively, for the phase with $x=0.17$. As the ions occupy more and

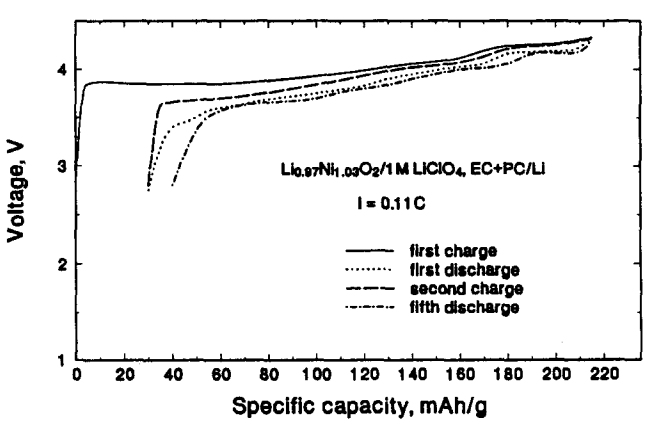


Fig. 3. Charge/discharge curves of $Li_{0.97}Ni_{1.03}O_2$ cathode in the first, second and fifth cycles at 0.5 mA/cm² in 1 M $LiClO_4$, EC–PC.

more sites in the crystal lattice of $LiNiO_2$ the diffusion polarization in the solid phase grows to reach a considerable value of ~1 V at the end of the discharge where $x=0.80$.

Three well-expressed voltage plateaus are manifested in the charge/discharge curves at 3.5, 3.6, 4.0 and 4.2 V, respectively, which reflect the phase transitions in the compounds. They coincide well with those determined more precisely by Ohzuku et al. [3] by means of open-circuit potential versus $x$ plots.

The coulombic efficiency in the first cycle $(CE)_1 = q_d/d_c$ in the example, shown in Fig. 3, is 87% but in general it varies from 75 to 87% depending on the value of $x$ and on the cycling conditions. The large initial charging capacity is very appropriate for the Li-ion cells since the high capacity carbon anodes (250–320 mAh/g) can be fully charged in the first cycle with a smaller excess of the cathode material. The coulombic efficiency $(CE)_n$ steeply increases in the first three to six cycles and reaches a comparatively stable value of $99.1 \pm 0.4\%$. The capacity loss of ~0.9% at each charge is most likely consumed for the electrolyte oxidation at high anodic potentials on the cathode surface.

On the other hand, the cycling stability of the cathode (CS) is determined from the decay of the discharge capacity with the number of cycles by the expression proposed by Yamaki et al. [13]:

$$(q_d)_n = (q_d)_m(CS)^{n-m} \quad (1)$$

under the assumption that (CS) is constant; $m$ is the number of cycles during the initial steep decay of the capacity where (CS) is decreasing (usually $m=5$), and $n$ is the number of the last cycle in the test. Fig. 4 exhibits the results of a cycling test of a cathode cycled at 0.48 mA/cm between 2.6 and 4.25 V of a sample with $x=0.974$. The (CS) value estimated by Eq. (1) yield 99.88% which shows that the discharge capacity loss is only 0.12% per cycle, much lower than that of the coulombic efficiency, 0.9%.

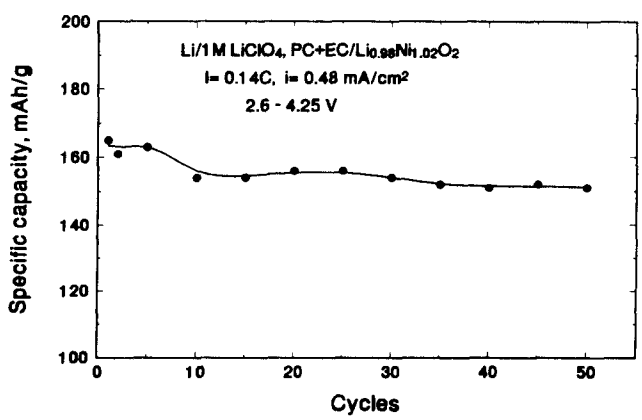


Fig. 4. Decrease in the discharge capacity during cycling of a $Li_{0.99}Ni_{1.01}O_2$ cathode cycled between 2.60 and 4.25 V in a 1 M $LiClO_4$, EC–PC electrolyte at 0.48 mA/cm$^2$.

It was of interest to relate the charge and discharge capacity in the first cycle with the value of $x$. The plots in Fig. 5 reveal the expected rise of both $q_c$ and $q_d$ up to $x \approx 0.97$, where a flat maximum is reached followed by a rather unexpected decrease in the 0.98–0.99 range. The unexpected maximum in the capacity versus $x$ dependence at $x=0.97$–$0.98$ could find a plausible explanation in the maximum of the chemical diffusion coefficient, $D$, of $Li_xNiO_2$ at $x=0.95$ reported by Bruce et al. [14]. With the rise of $x$ from 0.95 to 0.99, the maximum of $D$ is followed by a steep decrease by about 3 orders of magnitude.

The charging curves in Fig. 3 indicate that the cathode capacity is rather sensitive to the end charge voltage. This is corroborated by plots in Fig. 6 for a sample with $x=0.974$. The capacity rise in the 4.2–4.3 V range is steep, whereafter a saturation value is attained. In contrast, the sample with $x=0.989$, exhibiting no clear voltage plateau at the end of the charging curve, shows a lower and more uniform slope in the $q$ versus $x$ plots in Fig. 6.

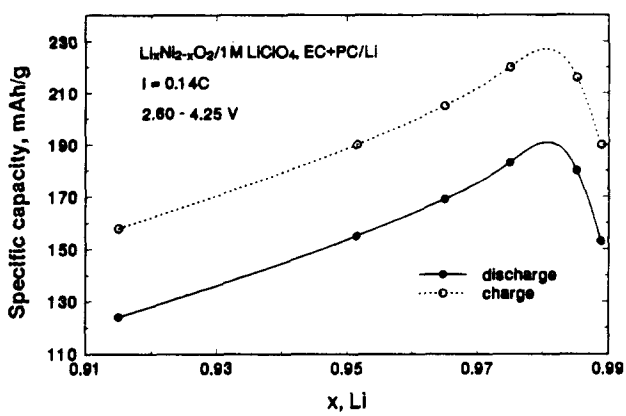


Fig. 5. Effect of $x$ in the $Li_xNi_{2-x}O_2$ phase on (O) charge and (●) discharge capacity in the first cycle.

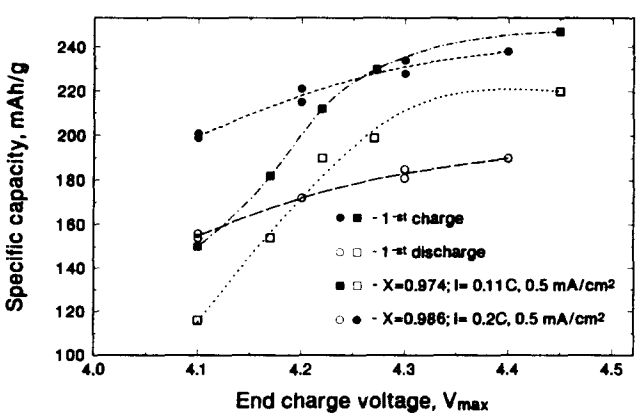


Fig. 6. Effect of the maximum charging voltage $U_{max.}$ on the charge and discharge capacity in the first cycle, discharged to 2.6 V at 0.48 mA/cm$^2$ in 1 M $LiPF_6$, EC–PC electrolyte of $Li_xNi_{2-x}O_2$ cathodes with $x=0.974$ and $x=0.989$.

## References


[1] T. Nagaura, *Prog. Batteries Battery Mater., 10* (1991) 209.
[2] K. Sekai, H. Azuma, A. Omaru and S. Fujita, *J. Power Sources, 43/44* (1993) 241.
[3] T. Ohzuku, A. Ueda, M. Nagayama, Y. Iwakoshi and H. Komori, *Electrochim. Acta, 38* (1993) 1159, and refs. therein.
[4] J. Dahn, U. von Sacken,M. Juzkow and H. Janaby, *J. Electrochem. Soc., 138* (1991) 2207, and refs. therein.
[5] J. Dahn, U. von Sacken and C. Michal, *Solide State Ionics, 44* (1990) 87.
[6] T. Ohzuku, A. Ueda and M. Nagayama, *J. Electrochem. Soc., 140* (1993) 1862.
[7] H. Arai, S. Okada, H. Ohtsuka and M. Ishimura, *Proc. Symp. New Sealed Rechargeable Batteries,* Proc. Vol. 93-23, The Electrochemical Society, Pennington, NJ, USA, p. 452.
[8] D. Guyomard and J. Trascon, *J. Electrochem. Soc., 139* (1992) 937.
[9] A. Momchilov, V. Manev and A. Kozawa, *J. Power Sources, 41* (1993) 305.
[10] D. Guyomard and J. Tarascon, *US Patent No. 5 192 629* (1993).
[11] J. Morales, C. Peres-Vicente and J. Tirado, *Mater. Res. Bull., 25* (1990) 623.
[12] J. Reimers, J. Dahn, J. Greedan, C. Stager, G. Lui, I. Davidson and U. von Sacken, *J. Solid State Chem., 102* (1993) 542.
[13] J. Yamaki and A. Tobishima, *Electrochim. Acta, 35* (1990) 383.
[14] P. Bruce, A. Lisowska-Oleksiak, M. Saidi and C.A. Vincent, *Solid State Ionics, 57* (1992) 353.